Regulation of the Enzymatic Catalysis of Poly(ADP-ribose) Polymerase by dsDNA, Polyamines, Mg^{2+}, Ca^{2+}, Histones H_1 and H_3, and ATP†

Ernest Kun,*,‡ Eva Kirsten,§ Jerome Mendeleyev,§ and Charles P. Ordahl*,§

Departments of Anatomy and Cellular and Molecular Pharmacology and The Cardiovascular Research Institute, University of California, San Francisco, California 94143

Received July 25, 2003; Revised Manuscript Received October 20, 2003

ABSTRACT: The enzymatic mechanism of poly(ADP-ribose) polymerase (PARP-1) has been analyzed in two *in vitro* systems: (a) in solution and (b) when the acceptor histones were attached to a solid surface. In system (a), it was established that the coenzymatic function of dsDNAs was sequence-independent. However, it is apparent from the calculated specificity constants that the AT homopolymer is by far the most effective coenzyme and randomly damaged DNA is the poorest. Rates of auto(poly-ADP-ribosylation) with dsDNAs as coenzymes were nearly linear for 20 min, in contrast to rates with dcDNA, which showed product [$(ADPR)_n$] inhibition. An allosteric activation of auto(poly-ADP-ribosylation) by physiologic cellular components, Mg^{2+}, Ca^{2+}, and polyamines, was demonstrated, with spermine as the most powerful activator. On a molar basis, histones H_1 and H_3 were the most effective PARP-1 activators, and their action was abolished by acetylation of lysine end groups. It was shown in system (b) that oligo(ADP-ribosyl) transfer to histone H_1 is 1% of that of auto(poly-ADP-ribosylation) of PARP-1, and this trans-(ADP-ribosylation) is selectively regulated by putrescine (activator). Physiologic cellular concentrations of ATP inhibit PARP-1 auto(poly-ADP-ribosylation) but less so the transfer of oligo(ADP-ribose) to histones, indicating that PARP-1 auto(ADP-ribosylation) activity is dormant in bioenergetically intact cells, allowing only trans(ADP-ribosylation) to take place. The inhibitory mechanism of ATP on PARP-1 consists of a noncompetitive interaction with the NAD site and competition with the coenzymic DNA binding site. A novel regulation of PARP-1 activity and its chromatin-related functions by cellular bioenergetics is proposed that occurs in functional cells not exposed to catastrophic DNA damage.

Poly(ADP-ribose) polymerase (PARP-1, EC 2.4.2.30) is a highly abundant non-histone protein component of all eukaryotes (above *Saccharomyces*), which, besides its association with chromatin, possesses the enzymatic activity to transfer adenosine diphosphoribose from NAD to various acceptor proteins. Both the biological significance of this covalent protein-modifying reaction and the dependence of PARP-1 on damaged DNA have been the subject of numerous publications (*1*, *2*), but no distinct cellular physiologic function of PARP-1 has as yet been defined, relegating PARP-1 to pathophysiology.

The notion that broken DNA is an essential coenzyme of PARP-1 is based on early observations of Benjamin and Gill (*3*), who showed a strong stimulation of PARP-1 activity by DNAase 1-treated dsDNA.[1] Under these circumstances, PARP-1 transfers ADP-ribose polymers (>20 subunits) to other PARP-1 molecules [auto(poly-ADP-ribosylation)] (*4*). Subsequent results of Zahradka and Ebisuzaki (*5*) demonstrated a Zn^{2+} requirement for PARP-1 activity, and extensive work from DeMurcia's laboratory (*6*) provided strong evidence for the participation of two "asymmetric" Zn^{2+} fingers in PARP-1. It was known that proteins containing "symmetric" Zn^{2+} fingers, where all four Zn^{2+} coordinations take place with cysteine residues (*7*), bind to DNA largely by way of DNA sequence specific interactions. The anomaly of PARP-1 Zn^{2+} fingers, which appear to bind to single-stranded DNA breaks independent of the DNA nucleotide sequence (*6*), remained unexplained in terms of molecular mechanisms, even though the asymmetry of PARP-1 Zn^{2+} fingers (containing one histidine residue and three cysteine residues) was known. Therefore, we cannot strictly exclude the possibility that "nonspecifically" produced single-stranded DNA termini may coordinate with Zn^{2+} in asymmetric Zn^{2+} fingers, as in PARP-1, by replacing histidine as a Zn^{2+} ligand. Such a reaction mechanism would require single-strand breaks in dsDNA, but leaves the physiologic meaning of this reaction undetermined.

In a preceding report (*4*), we presented evidence that end-protected dsDNAs, originally derived from MCAT-containing elements (*8*−*10*), which have no DNA breaks, were more effective coenzymes of PARP-1, especially in histone H_1-activated systems, than randomly damaged DNA. Under these circumstances of auto- or trans-modification of histone

† This work was supported by NIH Grants HL59693 and HL35561 to C.P.O.

* To whom correspondence should be addressed. Telephone: (415) 476-4051. Fax: (415) 476-4845. E-mail: cmkun@comcast.net (E. Kun) and ordahl@itsa.ucsf.edu (C.P.O.).

‡ Department of Cellular and Molecular Pharmacology.

§ Department of Anatomy and The Cardiovascular Research Institute.

[1] Abbreviations: dsDNA, double-stranded DNA; dcDNA, discontinuous DNA (DNA damaged by DNAase I, alkylation agents, or radiation); ADPR, adenosine diphosphoribose [$(ADPR)_n$ is an oligomer of ADPR]; TOPO I, topoisomerase I; AMP-PNP, β-γ-imidoadenosine 5′-triphosphate; MNNG, 1-methyl-*N*′-nitro-*N*-nitrosoguanidine; PBS, phosphate-buffered saline that is free of Ca^{2+} and Mg^{2+}.

10.1021/bi0301791 CCC: $27.50
Published on Web 12/13/2003

H_1, or other acceptors, relatively short chains (<20 subunits) are synthesized, which herein is termed "oligo(ADP-ribosylation)". These results with dsDNA coenzymes pointed toward a physiological role of PARP-1 in cell function. Following this lead, this report deals with the analysis of the effect of varying DNA sequences of dsDNAs as coenzymes of PARP-1. Since Mg^{2+} exerted significant regulation of PARP-1 (*4*), we extended our study to other physiologically occurring cations (Ca^{2+}, polyamines, and histones H_1 and H_3) and to ATP, the generally recognized central molecule of cellular bioenergetics. All of these physiologic cellular constituents had characteristic effects on PARP-1, thereby establishing a biologically meaningful enzyme control that is being extended to a cellular level.

MATERIALS AND METHODS

The sources of PARP-1 and histones H_1 and H_3 as well as of other reagents and methods were the same as reported previously (*4*). Comparison of K_{cat} and K_m (see pages 99−109 of ref *11*) values obtained with dsDNAs with varying sequences was performed in the "soluble assay" system (50 μL, pH 8.0) as reported previously (*4*). The quantitative analysis of PARP-1- and histone H_1-bound oligo-ADPR was carried out as described below.

Simultaneous quantitative oligo- and poly(ADP-ribosylation) of both histone H_1 and PARP-1 proteins was assayed in a 96-well plate as described previously (*4*), except biotinylated NAD was replaced with [^{32}P]NAD as follows. Wells were coated with 50 μL (per well) of a histone H_1 solution in PBS (100 μg/mL) at 4 °C overnight. The wells were then dried by tapping them on paper towels and rinsed with 5 × 100 μL of PBS, and the reaction mixture was added to tap-dried wells consisting of 5 μL of 100 nM dsDNA, 5 μL of H_2O (or 250 mM $MgCl_2$ or 30 mM spermine), 2.5 μL of 1 M Tris-HCl (pH 8.0), 0.5 μL of PARP-1 (100 μg/mL, to give a final concentration of 8 nM), and 17 μL of H_2O (per well). The reaction was started with 20 μL of 1 mM NAD (containing ^{32}P label to give ~1 × 10^6 dpm/well), and then the mixture was incubated for 10−20 min at room temperature. The reaction was terminated by siphoning off 50 μL of supernatant (containing PARP-1) and delivering it into 900 μL of 25% TCA (in Eppendorf vials) followed by a 50 μL PBS rinse of the well. To remove remaining traces of soluble radioactivity, this step was followed with five washes with 100 μL of PBS each, and the washes were discarded. To the supernatant as a coprecipitant was added 40 μL of BSA (10 mg/mL); the tubes were vortexed and centrifuged for 10 min at 4 °C, and after removal of the TCA supernatant, the precipitate was washed three times with 900 μL of 20% TCA. The radioactivity of the TCA precipitate was determined by placing the precipitate-containing tubes into scintillation vials filled with scintillation fluid, followed by scintillation spectrometry.

The quantity of histone H_1 or H_3 bound to each well was determined by the Bio-Rad protein test before and after the coating procedure; the attached amount was calculated from the difference, and the amount of covalently attached oligo-ADPR was calculated per picomole of histones (or picomole of PARP-1 in the supernatant). The amount of [^{32}P]ADP-ribose bound to histone H_1 was determined by treating the attached histone H_1 with 50 μL of 1 N NaOH at 37 °C for 1 h, dislodging it by repeated pipetting, and then determining the amount of ^{32}P by transferring the material to counting vials with one wash with 50 μL of 1 N NaOH. The net histone-bound $(ADPR)_n$ counts were obtained by subtracting counts from noncoated wells, representing the background.

The lysine end groups of histones H_1 and H_3 were acetylated by the method of Fraenkel-Conrat (*12*) as follows. Histones (5 mg) were dissolved (or suspended in the case of H_3) in 200 μL of half-saturated sodium acetate in 1 mL glass reaction vials chilled in an ice bath. Acetic anhydride was added in three 2 μL portions, spaced 20 min apart over the course of 1 h. The reaction mixture was vortexed after each addition and kept chilled in the ice bath. It was then dialyzed at 4 °C against distilled water (2 h) and PBS (2 h). The dialysate was transferred to a vial; PBS was added to a final volume of 1 mL, and the protein was quantitated by the Bradford method (Bio-Rad).

Steady state velocity constants were calculated from Lineweaver−Burk plots (see pages 38−50 of ref *13* and pages 99−109 of ref *11*) carried out in triplicate, where deviations were within ±10% of the mean. Nonlinear (sigmoidal) regression curves were obtained by plotting reaction rates at varying concentrations of the bivalent cations using SigmaPlot and curve fitting by a standard sigmoidal curve fitting equation (99% confidence). Hill coefficients were directly read from slopes of linear plots according to the equation (see pages 165 and 166 of ref *13*) $\log[v/(V_s - v)]$ versus $\log(L)$.

RESULTS

Effect of Nucleotide Sequences of dsDNAs. The histone H_1-stimulated oligoadenosine diphosphoribose transferase reaction, which includes histone-stimulated auto(ADP-ribosylation) and trans(ADP-ribosylation) to histone H_1, was characterized by K_{cat} and K_m values determined under conditions reported previously (*4*). As shown in part A of Table 1, experiments 1 and 2 included nucleotides that also test positively in the differentiation assay, but experiments 4−7 included compounds, while serving as coenzymes in the enzymatic test, that have no function in differentiation. Damaged DNA (dcDNA) (experiment 4) has the lowest K_{cat}, whereas the AT homopolymer exhibits the highest apparent affinity. Various preparations of dcDNA as a coenzyme tend to exhibit variable degrees of coenzymic action, in contrast to dsDNAs, which are constant. Column 3 of Table 1 lists "specificity constants" of PARP-1-catalyzed reactions as influenced by dsDNAs of varying composition compared with dcDNA. This constant, as defined by Fersht (*11*), is the K_{cat}/K_m ratio, being equal to v which holds true at any substrate concentration and is related to the apparent second-order rate constant of the forward reaction pathway. Therefore, the K_{cat}/K_m value can serve as an indicator of the catalytic efficacy of DNAs, keeping all other variables constant. As seen from Table 1 (column 3), the AT homopolymer is by far the most effective coenzyme and dcDNA the weakest. This is also consistent with, and supports, earlier results (*4*).

A further significant difference between the coenzymic function of dsDNAs and dcDNA is the maintenance of nearly linear rates of poly(ADP-ribosylation) for 20 min by dsDNA but not by dcDNA. This is illustrated in Figure 1A, where

Table 1: Catalytic Constants of dsDNAs with Varying Nucleotide Sequences[a]

	nature of the DNA coenzyme	K_{cat}	K_m	K_{cat}/K_m ($\times 10^{-3}$)
	(A) Histone H_1-Supported Poly(ADP-ribosylation) Reactions			
1	MCAT-1 (end-protected)	2.50	45	55
2	MCAT-1 (free ends)	1.75	26	67
3	SV40 MCAT (end-protected)	2.50	45	45
4	dcDNA (damaged DNA)	0.75	26	29
5	NSC	2.50	24	101
6	AT homopolymer (end-protected)	2.50	10	250
7	CG homopolymer (end-protected)	1.56	20	78
	(B) Mg^{2+}-Supported Poly(ADP-ribosylation) Reactions			
1	MCAT-1 (end-protected)	2.50	400	6.2
2	MCAT-1 (free ends)	1.90	~400	4.7
3	dcDNA (damaged DNA)	3.10	~500	6.9
4	AT homopolymer (end-protected)	7.5	85	88
5	GC homopolymer (end-protected)	1.5	85	18

[a] Varied concentrations of the DNA coenzymes (5−40 nM) were used to determine K_{cat} (nanomoles of ADP-ribose bound per milliliter per picomole of PARP-1) and K_m (nanomoles of dsDNA or equivalent weight of dcDNA) values from double-reciprocal plots (see Materials and Methods). The amount of ADP-ribose bound to protein was determined from the acid-precipitable radioactivity derived from [^{32}P]NAD. Poly(ADP-ribosylation) reaction mixtures in the presence of histone H_1 (50 μL) contained 5 μg of histone H_1 and 8 nM PARP-1. Auto(poly-ADP-ribosylation) reaction mixtures (50 μL) contained 32 nM PARP-1 and 25 mM Mg^{2+} but lacked histone. NSC nonspecific control oligonucleotide (5′-TGGTCGTATCTTCACCGTATCTG-3′) with free ends.

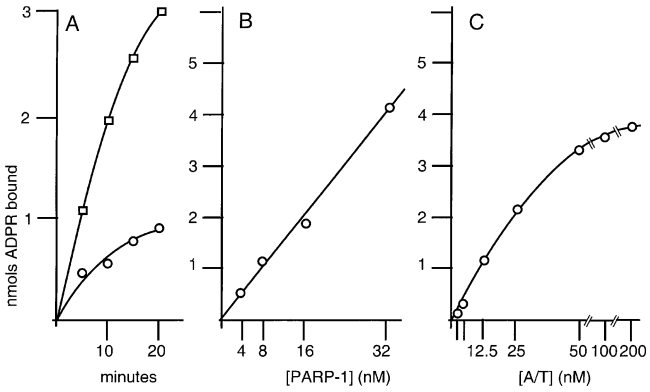

FIGURE 1: Effects of time and concentration on auto(poly-ADP-ribosylation). (A) Time linearity of ADP-ribosylation activated by 20 nM end-protected AT 23mer (□) or by randomly broken (nuclease 1-treated) salmon sperm DNA (○) (10 μg/50 μL assay) in the presence of 2.4 μM histone H_1 and 8 nM PARP-1. (B) Dependence of the rate of ADP-ribosylation on the concentration of PARP-1 in the range of 4−32 nM in the presence of 100 nM end-protected AT 23mer and 25 mM $MgCl_2$. (C) Rate of ADP-ribosyalation in the presence of 32 nM PARP-1 and 3 mM spermine with varied concentrations of end-protected AT 23mer. All reactions (50 μL) were performed in the soluble system by the second method outlined in ref *4*. Enzyme assays were carried out in triplicate where variations from the mean value did not exceed ±10%.

the catalytic activity of 8 nM PARP-1 is measured with 20 nM dsDNA (or dcDNA at 10 μg/50 μL) added in amounts conventionally applied in PARP-1 assays. The generally experienced self-inhibition of PARP-1 by auto(poly-ADP-ribosylation) in the presence of broken DNA as a "coenzyme" is clearly avoided by dsDNA (Figure 1A). The reaction rate with dsDNA as the coenzyme is proportional to the quantity of PARP-1 protein (Figure 1B) and shows saturation with dsDNA (Figure 1C). It can be concluded that while no correlation was found between the nucleotide sequence and coenzymic function, quantitative differences

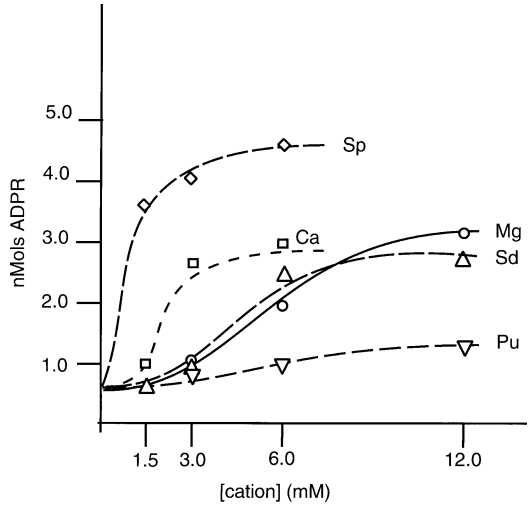

FIGURE 2: Cationic effects on auto(poly-ADP-ribosylation). The activating effects of cations on auto(poly-ADP-ribosylation) were tested in the soluble assay system (*4*) containing 200 nM dsDNA (AT 23mer, end-protected), 32 nM PARP-1, the indicated ions (Sp, spermine; Ca, calcium; Mg, magnesium chloride; Sd, spermidine; and Pu, putrescine), and 400 μM [^{32}P]NAD (pH 7.3) incubated in a total volume of 50 μL for 10 min at room temperature (20 °C), followed by determination of acid precipitable radioactivity. Averages from triplicate measurements are shown; the error range was ±10%.

in the catalytic efficacy of dsDNAs with varying compositions are observed for both K_{cat} and K_m.

The Mg^{2+}-stimulated auto(ADP-ribosylation) reaction (part B of Table 1) was also most efficiently catalyzed by the AT homopolymer as the coenzyme and least by the dcDNA. MCAT-1 exhibited much lower K_{cat} and K_m values than the AT homopolymer. Just like the histone H_1-activated reaction (Table 1A), no sequence specificity for coenzymic DNA was apparent, but the efficacy of catalysis was influenced by the nature of the DNA.

Effects of Polyamines, Ca^{2+}, and Mg^{2+} on the Auto-Poly-(adenosine diphosphoribose) Transfer Reactions Determined in the Soluble Assay System. The correlation between the concentration of cations and rates of auto(poly-ADP-ribosylation) at pH 7.3 is summarized in Figure 2. In Figure 2, the coenzymic DNA was 200 nM AT. Spermine proved to be the most powerful activating cofactor, disclosing the fact that the long-sought biologic mode of action of polyamines (*14*, *15*) is most probably the regulation of auto(ADP-ribosylation) of PARP-1. It is of special interest that whereas spermine exerts the largest increase in the level of auto(poly-ADP-ribosylation), putrescine is only 10% as active in the same reaction but is a far more effective activator in trans-(ADP-ribosylation) of histone (see below and Figure 7). Spermidine is less effective than spermine (Figure 2). It follows that both auto- and trans(ADP-ribosylation) are differentially regulated by two members of the polyamine pathway (spermine and putrescine). Spermidine, Ca^{2+}, and Mg^{2+} followed spermine in activating potency. It is important to note that without the activating cations, coenzymic DNAs had a negligible effect on auto(ADP-ribosylation); therefore, not DNA *per se* but the activating cations and DNA are required for optimal enzymatic activity.

Allosteric Properties of PARP-1. Observing the sigmoidal kinetics of activation of auto(ADP-ribosylation) (Figure 2), we calculated Hill coefficients (see Materials and Methods)

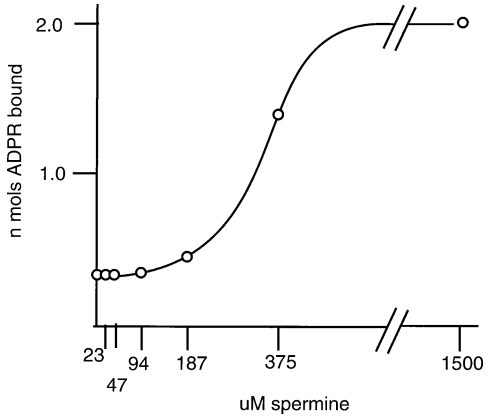

FIGURE 3: Effect of spermine, over an expanded concentration range, on auto(poly-ADP-ribosylation). Incubation was as described in the legend of Figure 2, except that 100 nM dsDNA (AT 23mer) was used with the addition of the indicated varied concentrations of spermine. Values are the average of triplicate measurements that were within ±10% of the mean.

for the bivalent cation-dependent reactions. Expanding the concentration range of spermine (Figure 3), we obtained Hill coefficients of 11 for spermine, 6 for Ca^{2+}, and 2 for Mg^{2+}, calculated from Figure 2. These unexpectedly high apparent cooperative kinetics strongly suggest that PARP-1 is not simply a regulatory enzyme catalyzing the polymerization of ADP-ribose, but that as a protein structure also undergoes oligomerization itself. Kinetic evidence for the oligomerization of PARP-1 has been obtained during studies concerned with the activating action of PARP-1 on Topo I (*16*), and the large Hill coefficient, particularly with the polyamine, spermine (Figure 3), indicates a macromolecular association of PARP-1, a new observation requiring further studies.

Activating Effect of Histones H_1 and H_3 on Auto-Oligoadenosine Diphosphoribose Binding to PARP-1. Histone H_1, which in solution is both a PARP-1 activator and an ADP-ribose acceptor (*17*), is approximately twice as effective as histone H_3, but acetylation of both histones abolishes catalytic activation (Figure 4). This result identifies the basic lysine end groups of histones H_1 and H_3 as the most probable activating molecular species. On a molar basis, histones are $\sim 10^3$ more potent activators of PARP-1 than bivalent cations (compare with Figures 2 and 4). This effect is likely to represent a novel catalytic role of histones in cell physiology. It is important that the histone-activated systems show no cooperative kinetics. The increased rate of poly(ADP-ribosylation) in the presence of histone H_1 versus that in the presence of H_3 (Figure 4) is most probably due to the catalytic activity of histone H_1 being intrinsically higher than that of H_3, not to the simultaneously occurring trans(ADP-ribosylation) to histone H_1. As could be predicted, 6 mM EDTA abolishes the activating effects of Ca^{2+} and Mg^{2+} (between 1 and 6 mM), but has no effect on the polyamine- or histone-induced activation of ADP-ribose transfer (not shown).

Mutual Effects of Activators. When low concentrations of Ca^{2+}, Mg^{2+}, or spermine are added together to the soluble auto-oligo(adenosine diphosphoribose transferase) assay system in amounts which by themselves cause only a small activation, their combined action induces more than additive augmentation (Figure 5). These results have significant physiologic and pharmacologic implications because hormones and drugs that modify cellular Ca^{2+}, Mg^{2+}, and polyamine content in concert can markedly influence the PARP-1 system, mediating direct effects of hormone and drug on chromatin function.

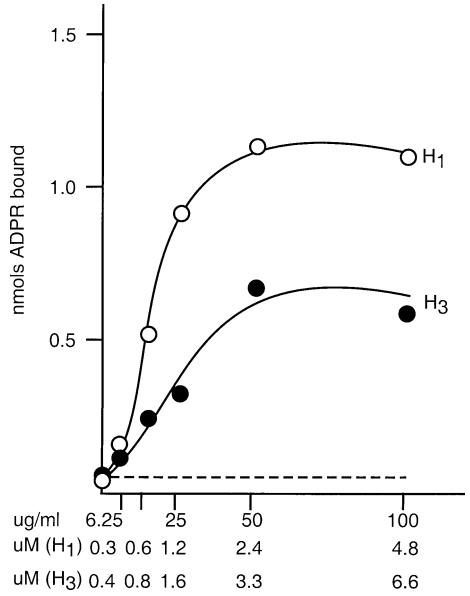

FIGURE 4: Histones as activators of PARP-1 activity. The activating effects of histones H_1 and H_3 on ADP-ribosylation were tested in the soluble assay system (total volume of 50 mL) containing 20 nM AT 23mer (end-protected), 8 nM PARP-1, and histones at the indicated concentration. Incubation and processing were as described in the legend of Figure 2. The dashed line indicates the absence of activation by acetylated histones H_1 and H_3. Values are the average of triplicate measurements that were within ±10% of the mean.

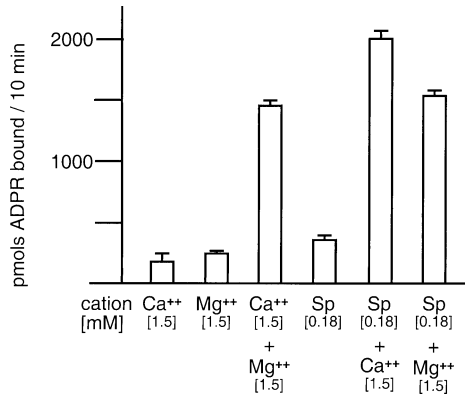

FIGURE 5: Combinatorial effects of cations on PARP-1 activity. Activating effects of low concentrations of calcium or magnesium alone or in combination, and those of a low spermine concentration alone or in combination with Ca^{2+} or Mg^{2+}, on auto(poly-ADP-ribosylation), tested in the soluble assay system with 20 nM AT (23mer, end-protected) and 32 nM PARP-1. Incubation and processing were as described in the legend of Figure 2. Error bars indicate the deviation from the mean in triplicate samples.

The apparent depression or inhibition of histone H_1-induced auto(poly-ADP-ribosylation) by 25 mM Mg^{2+} is illustrated in Figure 6. Whereas histone H_1 doubles the rate of auto(poly-ADP-ribosylation) of PARP-1 (compare bar 3 with bar 2) compared to that induced by Mg^{2+} alone, addition of Mg^{2+} to the histone-activated system abolishes the activation by histone H_1 (compare bar 4 with bar 3), indicating that Mg^{2+} at 25 mM competes with the activating action of histone H_1. This explains our previous results (*4*),

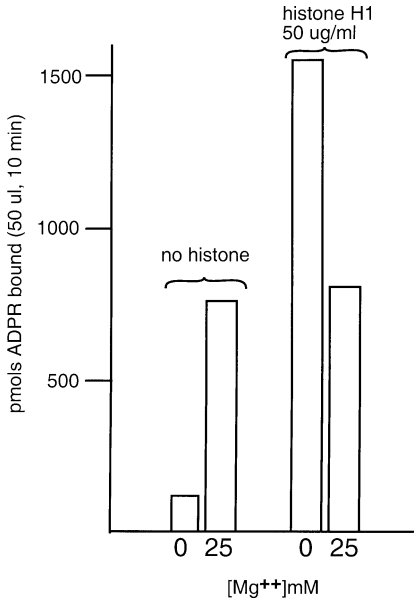

FIGURE 6: Combinatorial effect of Mg^{2+} and histone on PARP-1 activity. The effect of adding Mg^{2+} (25 mM) to a histone H_1-containing soluble assay system was tested and compared to the effect of adding Mg^{2+} to a histone-free soluble assay system (containing 8 nM PARP-1). Values are the average of triplicate measurements that were within ±10% of the mean.

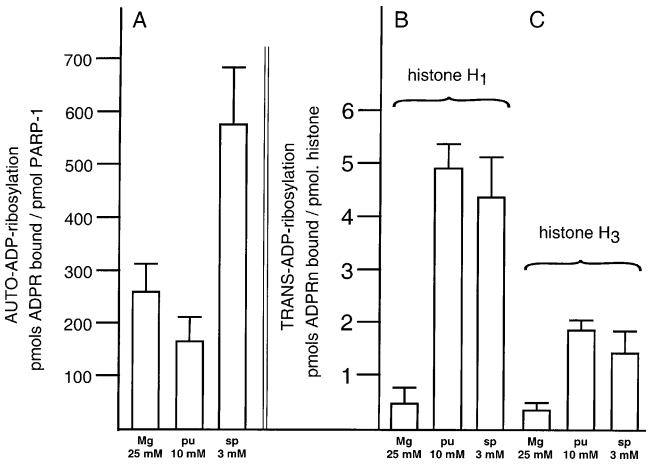

FIGURE 7: Cationic effects on simultaneous auto- and trans-modification by PARP-1 in a solid phase system. The wells of 96-well flat-bottom tissue culture plates were coated with histone H_1 (see Materials and Methods). After the wells were washed, a reaction mixture containing 10 nM dsDNA (GC 23mer, end-protected), 8 nM PARP-1, and the indicated ions was added to the wells, and the reaction was started by adding [^{32}P]NAD to give a final concentration of 400 μM. After incubation for 10 min at room temperature, auto(poly-ADP-ribosylation) (supernatant) and trans-(poly-ADP-ribosylation) (histone-attached) were assessed. Note the scale difference between panel A and panels B and C. Abbreviations are as described in the legend of Figure 2. Each bar shows the average of triplicate measurements that were within ±15% of the mean.

where addition of Mg^{2+} inhibits poly(ADP-ribosylation) in a histone H_1-activated system.

Quantitative Distribution of Covalently Bound Oligo(ADP-ribose) between PARP-1 and Histones. We have previously reported that histone H_1 attached to the wall of plastic wells serves as a direct acceptor for trans(ADP-ribosylation) from NAD to the histone protein, since PARP-1 (which is in solution) is quantitatively removed (*4*). This technique was extended to the simultaneous analysis of PARP-1- and histone-bound oligomers of ADP-ribose with the aid of [^{32}P]-NAD (see Materials and Methods). This "solid phase" assay may simulate physical conditions prevailing in cell nuclei, which have a high solute (protein or DNA) content that is not comparable with that in conventional assays performed in solutions. Both "solution" and solid phase assays represent enzymological models, requiring extension to cellular systems.

As shown in Figure 7, the quantity of ADP-ribose covalently bound to histone H_1 is only 1% of that bound to PARP-1; therefore, the increased rate with histone H_1 (Figure 6) can clearly be attributed to improved auto(poly-ADP-ribosylation) of PARP-1, assuming equivalent mechanisms in the "soluble" and "solid" state trans(ADP-ribosylation) assays. This assumption is supported by the fact that the same binding constants were obtained in both systems (*4*).

Results presented here with the aid of the solid phase assay provide the following information. As shown in Figure 7A, auto(poly-ADP-ribosylation) of PARP-1 in the presence of solid phase-attached histone H_1 and H_3 with 3 mM spermine as the maximal activator and dsDNA as the coenzyme yields 500 pmol of poly(ADP-ribose) synthesized per picomole of PARP-1 in 10 min. These polymers have long chains as deduced from the observed stoichiometry. With Mg^{2+} or putrescine, proportionately smaller quantities of polymers are synthesized, as predicted from Figure 2. However, simultaneous synthesis of histone H_1-bound oligomers (Figure 7B) shows that the extent of trans(oligo-ADP-ribosylation) to this protein is only 1% of the extent of auto(poly-ADP-ribosylation) with spermine as the activator and much less so with Mg^{2+}. In a comparison to the relatively weak activation of auto(ADP-ribosylation) of PARP-1 in the presence of putrescine, this diamine, which is the product of ornithine decarboxylase, appears to be relatively specific for the acceleration of trans(ADP-ribosylation) of histones, while spermine activates both auto- and trans(ADP-ribosylation).

As illustrated in Figure 7C, histone H_3, which is not poly-ADP-ribosylated in soluble assay systems (*17*), is covalently modified to a lesser extent (compared to histone H_1) when attached to the reaction well. This indicates that the modifiability by poly(ADP-ribosylation) of core histones, readily observed in nucleosomes, is imitated when core histones are bound to a solid surface.

Inhibition of PARP-1 by ATP. Results thus far obtained with *in vitro* enzyme systems constructed from PARP-1, dsDNA, cationic activators, and histones consistently show a large preference for auto(poly-ADP-ribosylation), as compared to histone H_1 trans(ADP-ribosylation), in agreement with general experience (*2*), but in variance with the protein-bound poly(ADP-ribose) content in intact animal tissues (*18*), which demonstrated only histone H_1 and some non-histone proteins as poly(ADP-ribose) acceptors *in vivo*. This apparent contradiction between *in vivo* and *in vitro* results is removed by the observation that ATP at physiologic concentrations preferentially inhibited auto(poly-ADP-ribosylation) (Figure 8A). Since aerobic metabolizing cells may contain ~10 mM ATP, we can predict that auto(poly-ADP-ribosylation) in aerobic, bioenergetically coupled cells is completely absent *in vivo*. However, trans(ADP-ribosylation) to histone H_1 was far less sensitive to inhibition by ATP (Figure 8B). Thus, in agreement with *in vivo* results

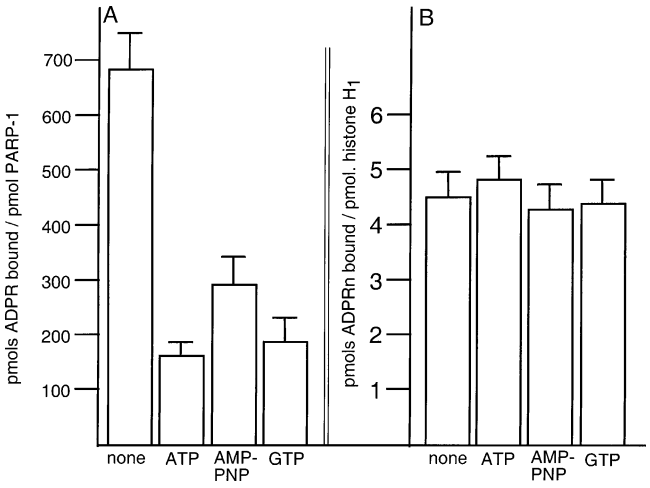

FIGURE 8: Effect of nucleotide triphosphates on PARP-1 activity. The differential effects of ATP, the nonhydrolyzable ATP analogue, AMP-PNP, and GTP (all at a concentration of 4 mM) on auto(poly-ADP-ribosylation) and trans(oligo-ADP-ribosylation) (A and B, respectively) were tested in the solid phase system. Each bar shows the average of triplicate measurements that were within ±15% of the mean.

Table 2: Effect of ATP on Spermine- and Histone-Stimulated Auto(poly-ADP-ribosylation)[a]

	[ATP] (mM)	ADPR bound (pmol)	inhibition (%)
spermine (3 mM)	0	1630	−
	1	1630	−
	2	1195	−28
	4	381	−77
	10	95	−94
histone H_1 (2.5 μM)	0	1660	−
	1	1216	−27
	2	1118	−33
	4	789	−53
	10	409	−76

[a] The effect of varied concentrations of ATP (from a 100 mM stock solution, lithium salt, Roche) on the rate of auto(poly-ADP-ribosylation) activated by 20 nM end-protected AT 23mer and (A) 3 mM spermine or (B) 2.5 μM histone H_1, with 8 nM PARP-1 (in both cases), was tested in the 50 μL soluble system (second method in ref *4*). The deviation from the mean of three parallel assays was ±4%.

(*18*), trans(ADP-ribosylation) is the most likely physiologic enzymatic process catalyzed by PARP-1 *in vivo* in normal cells. The inhibitory effect of ATP on auto(poly-ADP-ribosylation) of PARP-1 is shown in the soluble assay in Table 2. GTP and the nonhydrolyzable ATP analogue, AMP-PNP (Figure 8), also inhibit auto(poly-ADP-ribosylation) of PARP-1, while ADP and AMP have no effect (not shown). Since GTP is present at a far lower cellular concentration than ATP, the physiologic significance of ATP as a PARP-1 inhibitor prevails. In addition, these results also illustrate that ATP, not its dephosphorylated products, is the proper PARP-1 inhibitor.

The kinetics of inhibition of PARP-1 by ATP are illustrated in Figure 9 as Eadie−Hofstee plots. The inhibition by ATP is noncompetitive versus NAD but competitive with dsDNA. This complex interaction of ATP with PARP-1 involving both competitive and noncompetitive mechanisms at the enzymatic level requires further experimental work at a cellular level before a biochemical interpretation can be proposed. The competitive inhibitory constant for ATP versus

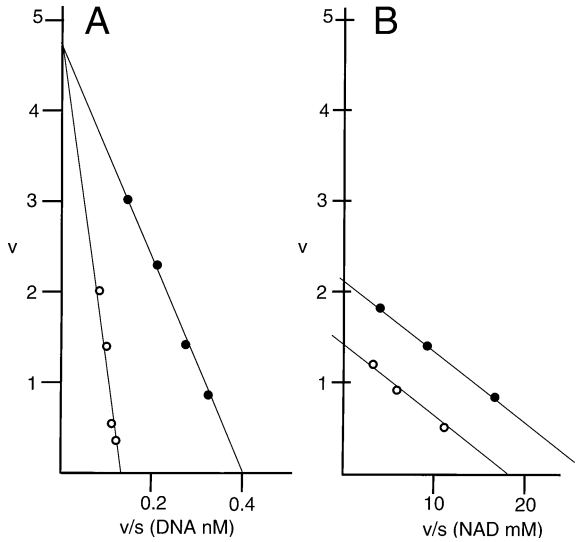

FIGURE 9: Kinetics of inhibition of PARP-1 activity by ATP. (A) The concentration of NAD was kept constant at 0.45 mM in a histone-supported soluble system assay containing (all concentrations are final) 50 mM Tris-HCl (pH 7.3), 8 nM PARP-1, and 2.5 μM histone H_1. The concentration of end-protected AT 23mer varied from 2.5 to 20 nM. Filled circles show the kinetics in the absence of ATP, while empty circles indicate the presence of 4 mM ATP. (B) As in panel A except that kinetics were measured at varied NAD concentrations of 50, 150, and 450 μM (all concentrations are final), in the absence (●) or presence (○) of 4 mM ATP. In both panels, the values represent averages from triplicate determinations that were within ±10% of the mean.

dsDNA is 2 mM, and 4 mM for the noncompetitive inhibition at the NAD site.

DISCUSSION

As seen from Table 1, the coenzymic function of dsDNAs is not strictly sequence specific, and thus, we have to assume that different molecular requirements exist for differentiation regulatory function of dsDNAs containing the MCAT motif. This subject is examined in the following paper (*30*).

There is a significant correlation between the effects of cations on the induced helical configuration of the poly(ADP-ribose) homopolymer (*19*, *20*) as measured by circular dichroism (CD) analyses and the activation of auto(ADP-ribosylation) (Figure 2). The coincidence of bivalent cation-induced CD signals and the activation of PARP-1 may indicate that the ADP-ribose oligomers in the helical configuration are the appropriate participants in poly(ADP-ribose) synthesis. Stockert (*21*) built a B-DNA−poly(ADP-ribose) model that demonstrates a steric fit between B-DNA and poly(ADP-ribose) in which a helix of poly(ADP-ribose) binds to the double helix of dsDNA in its minor groove. This theoretical triple-helix model is supported by the results of Minaga and Kun (*19*, *20*) which demonstrated the bivalent cation-induced helicity of poly(ADP-ribose), which is the prerequisite to Stockert's model. Formation of dsDNA−$(ADPR)_n$ triplexes may explain the absence of self-inhibition of poly(ADP-ribosylation) as shown in Figure 1.

It is presently unknown how the binding of a helical (ADPR) oligomer to dsDNA forming a dsDNA−$(ADPR)_n$ triplex contributes to the enzymatic mechanism of bivalent cation-promoted auto(poly-ADP-ribosylation) of PARP-1. However, it seems probable that this auto(poly-ADP-ribosylation) is biochemically distinct from trans(ADP-ribo-

sylation) to histones or to transcriptional factors since inhibition by ATP of the "auto" reaction can be nearly complete while the "trans" process is still sustained (Figure 7 and Table 2).

The activation of PARP-1 by Ca^{2+} connects to regulation in neuronal cells, where Ca^{2+} was shown to activate PARP-1 without DNA damage (*22*). The mitochondrial regulation of cellular Mg^{2+} (*23*) shows a mitochondrial metabolism-dependent control of PARP-1 by regulation of the cellular concentration of Mg^{2+}. The phenomenon of activation of PARP-1 by Mg^{2+} (*24*) and by spermine (*25*) has been observed with enzyme preparations where dcDNA was the coenzyme, and no regulatory significance of the cationic action of PARP-1 had been proposed.

The biologic significance of the results shown in Figures 8 and 9 cannot be overemphasized because it is apparent that all published results regarding PARP-1 activity in isolated nuclei or extracts are biased because the main cellular regulator, ATP, has been lost in the preparation of PARP-1 assay systems. The dormancy of PARP-1 in cells bioenergetically coupled by ATP explains the observation that a highly specific inhibitor of PARP-1, 6-amino-5-iodo-1,2-benzopyrone (*26*), has no perceptible pharmacologic action in normal cells, in contrast to bioenergetically malfunctioning cancer cells. The significance of this problem is the subject of ongoing work.

Induction of PARP-1 activity by relatively high concentrations of the alkylating agent MNNG (10^{-2}−10^{-1} M) or 3−9 Gy of radiation is frequently used to produce DNA damage in cellular systems to detect appreciable enzymatic activity (*2*). These concentrations are in sharp contrast to the concentration (0.7 μM) at which MNNG converts normal human fibroblasts to the malignant phenotype. At 0.7 μM, MNNG has no effect on DNA but uncouples oxidative phosphorylation and changes the cellular phenotype (*27*). The reversible decrease in the level of cellular ATP by the reversible uncoupling oxidative phosphorylation appears to be a feasible mechanism of cyclic activation of latent PARP-1 in contrast to invoking catastrophic cellular events by DNA fragmentation. Extension of this bioenergetic model to the regulation of PARP-1 is the subject of ongoing research.

The discovery of oligo(ADP-ribose) transferase activity in liver mitochondria (*28*) was recently confirmed by Du et al. (*29*), who also reported that mitochondrial PARP-1 plays a pivotal role in peroxynitrite-induced malfunction in neuronal cells. The direct involvement of ATP as a PARP-1 regulator, as shown here, provides the missing link in the cellular control by PARP-1, which functions also at a mitochondrial level.

ACKNOWLEDGMENT

We thank Nina Kostanian and Sharon Spencer for ongoing support.

REFERENCES

1. Althaus, F. R., and Richter, C. (1987) *Mol. Biol. Biochem. Biophys. 37*, 1−237.
2. deMurcia, G., and Shall, S. (2000) *From DNA-damage and stress signaling to cell death: poly ADP-ribosylation reactions*, Oxford University Press, New York.
3. Benjamin, R. C., and Gill, D. M. (1980) *J. Biol. Chem. 255*, 10502−10508.
4. Kun, E., Kirsten, E., and Ordahl, C. P. (2002) *J. Biol. Chem. 277*, 39066−39069.
5. Zahradka, P., and Ebisuzaki, K. (1984) *Eur. J. Biochem. 142*, 503−509.
6. Gradwohl, G., Menissier de Murcia, J. M., Molinete, M., Simonin, F., Koken, M., Hoeijmakers, J. H., and de Murcia, G. (1990) *Proc. Natl. Acad. Sci. U.S.A. 87*, 2990−2994.
7. Klug, A., and Rhodes, D. (1987) *Cold Spring Harbor Symp. Quant. Biol. 52*, 473−482.
8. Mar, J. H., and Ordahl, C. P. (1988) *Proc. Natl. Acad. Sci. U.S.A. 85*, 6404−6408.
9. Mar, J. H., and Ordahl, C. P. (1990) *Mol. Cell. Biol. 10*, 4271−4283.
10. Butler, A. J., and Ordahl, C. P. (1999) *Mol. Cell. Biol. 19*, 296−306.
11. Fersht, A. (1984) *Enzyme structure and mechanism*, W. W. Freeman and Co., New York.
12. Fraenkel-Conrat, H. (1957) *Methods Enzymol. 4*, 247−469.
13. Hammes, G. G. (1982) *Enzyme catalysis and regulation*, Academic Press, New York.
14. McCann, P., Pegg, A. E., and Sjoerdsma, A. (1987) *Inhibition of Polyamine Metabolism. Biological Significance and Basis for New Therapies*, Academic Press, New York.
15. Cohen, S. S. (1998) *A Guide to the Polyamines*, Oxford University Press, New York.
16. Bauer, P. I., Buki, K. G., Comstock, J. A., and Kun, E. (2000) *Int. J. Mol. Med. 5*, 533−540.
17. Buki, K. G., Bauer, P. I., Hakam, A., and Kun, E. (1995) *J. Biol. Chem. 270*, 3370−3377.
18. Minaga, T., Romaschin, A. D., Kirsten, E., and Kun, E. (1979) *J. Biol. Chem. 254*, 9663−9668.
19. Minaga, T., and Kun, E. (1983) *J. Biol. Chem. 258*, 725−730.
20. Minaga, T., and Kun, E. (1983) *J. Biol. Chem. 258*, 5726−5730.
21. Stockert, J. C. (1983) *J. Theor. Biol. 105*, 461−467.
22. Homburg, S., Visochek, L., Moran, N., Dantzer, F., Priel, E., Asculai, E., Schwartz, D., Rotter, V., Dekel, N., and Cohen-Armon, M. (2000) *J. Cell Biol. 150*, 293−307.
23. Kun, E. (1976) *Biochemistry 15*, 2328−2336.
24. Kawamura, M., Tanigawa, Y., Kitamura, A., Miyake, Y., and Shimoyama, M. (1981) *Biochim. Biophys. Acta 652*, 121−128.
25. Tanaka, Y., Hashida, T., Yoshihara, H., and Yoshihara, K. (1979) *J. Biol. Chem. 254*, 12433−12438.
26. Bauer, P. I., Kirsten, E., Varadi, G., Young, L. J., Hakam, A., Comstock, J. A., and Kun, E. (1995) *Biochimie 77*, 374−377.
27. Milo, G. E., Kurian, P., Kirsten, E., and Kun, E. (1985) *FEBS Lett. 179*, 332−336.
28. Kun, E., Zimber, P. H., Chang, A. C., Puschendorf, B., and Grunicke, H. (1975) *Proc. Natl. Acad. Sci. U.S.A. 72*, 1436−1440.
29. Du, L., Zhang, X., Han, Y. Y., Burke, N. A., Kochanek, P. M., Watkins, S. C., Graham, S. H., Carcillo, J. A., Szabo, C., and Clark, R. S. (2003) *J. Biol. Chem. 278*, 18426−18433.
30. Huang, K., Tidyman, W. E., Le, K.-U. T., Kirsten, E., Kun, E., and Ordahl, C. P. (2004) *Biochemistry 43*, 217−223.

BI0301791